Amino Acids
https://doi.org/10.1007/s00726-019-02731-4

ORIGINAL ARTICLE

Structure-guided approach to identify a novel class of anti-leishmaniasis diaryl sulfide compounds targeting the trypanothione metabolism

Gianni Colotti[1] · Francesco Saccoliti[3] · Marina Gramiccia[4] · Trentina Di Muccio[4] · Jay Prakash[5] · Sunita Yadav[6] · Vikash Kumar Dubey[6] · Giulio Vistoli[7] · Theo Battista[2] · Stefano Mocci[2] · Annarita Fiorillo[2] · Aasia Bibi[2] · Valentina Noemi Madia[3] · Antonella Messore[3] · Roberta Costi[3] · Roberto Di Santo[3] · Andrea Ilari[1]

Received: 18 January 2019 / Accepted: 3 April 2019

Abstract

Leishmania protozoans are the causative agent of leishmaniasis, a neglected tropical disease consisting of three major clinical forms: visceral leishmaniasis (VL), cutaneous leishmaniasis, and mucocutaneous leishmaniasis. VL is caused by *Leishmania donovani* in East Africa and the Indian subcontinent and by *Leishmania infantum* in Europe, North Africa, and Latin America, and causes an estimated 60,000 deaths per year. Trypanothione reductase (TR) is considered to be one of the best targets to find new drugs against leishmaniasis. This enzyme is fundamental for parasite survival in the human host since it reduces trypanothione, a molecule used by the tryparedoxin/tryparedoxin peroxidase system of *Leishmania* to neutralize the hydrogen peroxide produced by host macrophages during infection. Recently, we solved the X-ray structure of TR in complex with the diaryl sulfide compound RDS 777 (6-(sec-butoxy)-2-((3-chlorophenyl)thio)pyrimidin-4-amine), which impairs the parasite defense against the reactive oxygen species by inhibiting TR with high efficiency. The compound binds to the catalytic site and engages in hydrogen bonds the residues more involved in the catalysis, namely Glu466′, Cys57 and Cys52, thereby inhibiting the trypanothione binding. On the basis of the RDS 777–TR complex, we synthesized structurally related diaryl sulfide analogs as TR inhibitors able to compete for trypanothione binding to the enzyme and to kill the promastigote in the micromolar range. One of the most active among these compounds (RDS 562) was able to reduce the trypanothione concentration in cell of about 33% via TR inhibition. RDS 562 inhibits selectively *Leishmania* TR, while it does not inhibit the human homolog glutathione reductase.

Keywords Trypanothione metabolism · Trypanothione reductase · Structure-based drug design · Diaryl sulfide inhibitors

Abbreviations

FAD	Flavin dinucleotide
GSSG	Oxidized glutathione
hGR	Human glutathione reductase

Handling Editor: E. Agostinelli.

✉ Andrea Ilari
andrea.ilari@uniroma1.it

Gianni Colotti
gianni.colotti@uniroma1.it

Roberto Di Santo
roberto.disanto@uniroma1.it

[1] Istituto di Biologia e Patologia Molecolari, Consiglio Nazionale delle Ricerche, IBPM-CNR, c/o Dip. Scienze Biochimiche Università Sapienza, P.le Aldo Moro 5, 00185 Rome, Italy

[2] Dip. Scienze Biochimiche, Università Sapienza, P.le Aldo Moro 5, 00185 Rome, Italy

[3] Dip. Chimica e Tecnologie del Farmaco, Istituto Pasteur-Fondazione Cenci Bolognetti, Università Sapienza, P.le Aldo Moro 5, 00185 Rome, Italy

[4] Dipartimento di Malattie Infettive, Istituto Superiore di Sanità Viale Regina Elena, 299, 00161 Rome, Italy

[5] Department of Biosciences and Bioengineering, Indian Institute of Technology Guwahati, Assam 981039, India

[6] School of Biochemical Engineering, Indian Institute of Technology (Banaras Hindu University) Varanasi, Varanasi 221005, India

[7] Dip. di Scienze Farmaceutiche, Università degli Studi di Milano, via Mangiagalli 25, 20133 Milan, Italy

Published online: 29 April 2019

IR	Infrared
NADPH	Reduced nicotinamide adenine dinucleotide
TR	Trypanothione reductase
TryS	Trypanothione synthetase
TS_2	Trypanothione [*N*1,*N*8-bis(glutathionyl) spermidine]
$T(SH)_2$	Reduced trypanothione
TXN	Tryparedoxin
TXNPx	Tryparedoxin peroxidase I
VL	Visceral leishmaniasis

Introduction

Leishmania parasites are the causative agent of leishmaniasis, a neglected tropical disease infecting numerous mammals including humans throughout the world. Human leishmaniasis consists of three major clinical forms: visceral leishmaniasis (VL), which is fatal if left untreated, cutaneous leishmaniasis, which can heal spontaneously but leaves disfiguring scars and mucocutaneous leishmaniasis, which is not self-healing and can potentially be fatal. VL, which is caused by *Leishmania donovani* in East Africa and the Indian subcontinent and by *Leishmania infantum* in Europe, North Africa, and Latin America, causes an estimated 60,000 deaths annually (Desjeux 2004; Hotez et al. 2012). *Leishmania* spp., together with other protozoan pathogens responsible for diseases such as sleeping sickness (*Trypanosoma brucei*) and Chagas disease (*Trypanosoma cruzi*), belong to the Trypanosomatidae (trypanosomatids) family. The therapy against the diseases caused by Trypanosomatidae, and in particular against VL, mainly relies on treatments implying the use of drugs such as antimony, amphotericin, paromomycin, miltefosine, aminoquinoline or sitamaquine, unsatisfactory in terms of their safety and efficacy (Burza et al. 2018). For these reasons there is an urgent need to find new drugs against these diseases, which affect mainly people living in tropical and subtropical countries that have inadequate research capacities and public health infrastructures. As recently suggested by Zulfiqar and colleagues, advances in this field can be achieved by targeting proteins essential for parasite survival but that are absent in the human host (Zulfiqar et al. 2017).

In contrast to the mammalian redox defense machinery that is based on glutathione, trypanosomatid parasites possess trypanothione [*N*1,*N*8-bis(glutathionyl)spermidine] (TS_2) as the main detoxifying agent against oxidative damage. This dithiol is synthesized by trypanothione synthetase (TryS) and is reduced to $T(SH)_2$ by the trypanothione reductase (TR). $T(SH)_2$ is then used by the couple tryparedoxin/tryparedoxin peroxidase I (TXN/TXNPx) to neutralize hydrogen peroxide produced by macrophages during infection (Fig. 1) (Colotti et al. 2013a; Ilari et al. 2017). It has

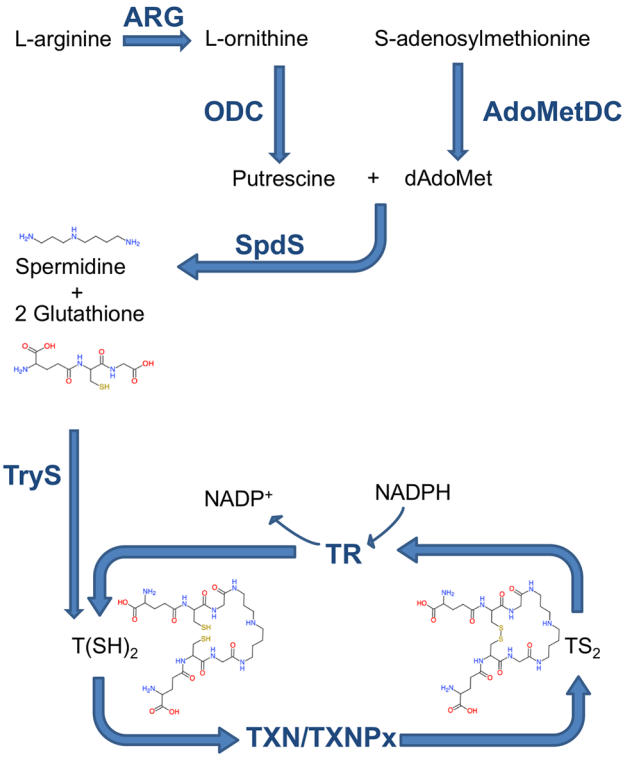

Fig. 1 Trypanothione metabolism. In the figure, the following abbreviations are used: *ARG* arginase, *ODC* ornithine decarboxylase, *AdoMetDC* *S*-adenosylmethionine decarboxylase, *SpdS* spermidine synthase, *TR* trypanothione reductase, *TryS* trypanothione synthetase, *TXN* tryparedoxin, *TXNPx* tryparedoxin peroxidase I, TS_2 trypanothione [*N*1,*N*8-bis(glutathionyl)spermidine], $T(SH)_2$ reduced trypanothione. The structure formulas of spermidine, glutathione and trypanothione are displayed

been shown that mutants displaying a partial trisomy of TR locus, where two TR alleles are disrupted by gene targeting, show attenuated infectivity and decreased ability to survive within the macrophages (Dumas et al. 1997). These data, together with the fact that all the attempts to date to obtain TR null mutants have failed, demonstrate that TR is an essential enzyme for the parasite survival. For this reason, this protein is an attractive target for the development of potential new drugs against trypanosomatids since it is also absent in the human host (Colotti et al. 2013a; Colotti and Ilari 2011). Indeed the human homolog, glutathione reductase (hGR), that maintains glutathione in a reduced state, displays a significantly different substrate binding site in terms of both volume and charge distribution, suggesting the possibility of identifying molecules able to selectively target TR (Colotti et al. 2013a).

The crystal structure of *L. infantum* TR (Baiocco et al. 2009a) that has been solved by Baiocco et al. is very similar to the structure of other trypanosomatid TRs solved to date, such as those from *Crithidia fasciculata*, *T. cruzi* and *T. brucei* (Bailey et al. 1993; Patterson et al. 2011;

Saravanamuthu et al. 2004). It is a twofold symmetrical homodimer in which each subunit is formed by three domains, i.e., the interface domain (residues 361–488), the NADPH-binding domain (residues 161–288) and the FAD binding domain (residues 1–160 and 289–360). The trypanothione binding site resides in a large cavity at the interface between the two monomers, formed by the residues of the FAD binding domain of one subunit and those of the interface domain of the other. The mechanism of trypanothione reduction catalyzed by TR involves NADPH, which transfers two electrons via FAD to the Cys52–Cys57 disulfide bridge. TS_2 then binds to the protein and Cys52, deprotonated by the couple His461′–Glu466′, nucleophilically attacks the trypanothione disulfide bridge with the formation of a mixed disulfide. Finally, the attack of Cys57 on Cys52 promotes the release of the reduced substrate (Baiocco et al. 2009a).

Antimony-containing drugs, still among the most used against VL, and other metals and metal-containing compounds can inhibit TR by binding to the two catalytic cysteines of the active site (Baiocco et al. 2011; Colotti et al. 2013b, 2018; Ilari et al. 2012, 2015). In addition to metal compounds, several organic compounds have been shown to inhibit TR activity by binding to the trypanothione binding site: 2-iminobenzimidazoles (Holloway et al. 2007), polyamine analogs (Dixon et al. 2005), quinoline-based compounds (Spinks et al. 2009), pyrimidopyridazine-based scaffolds (Spinks et al. 2009), azole-based compounds (Baiocco et al. 2013), lunarine analogs (Hamilton et al. 2006) and diaryl sulfides (Saccoliti et al. 2017; Stump et al. 2008) have all been reported. Some of these compounds were identified using high-throughput screenings, employing the colorimetric method for detection of TR activity (Martyn et al. 2007; Spinks et al. 2009) developed by Hamilton et al. (2003).

Recently our group identified among the GlaxoSmithKline LeishBOX, containing 192 molecules selected by high-throughput whole-cell phenotypic screening from a collection of 1.8 millions of compounds, carboxamide molecules able to selectively inhibit TR with high potency, not active on the human homolog glutathione reductase, and able to kill *Leishmania* parasites. Among them, the compound A1/7 (*N*-{4-methoxy-3-[(4-methoxyphenyl)sulfamoyl]phenyl}-5-nitrothiophene-2-carboxamide) is the only compound present also in the ChagasBOX and in the HATBOX, and for this reason, represents a lead compound to find new drugs against all the trypanosomatid diseases (Ilari et al. 2018). We were also able to develop a new luminescence-based assay to screen a library of 120,000 compounds, which allowed us to find new scaffolds able to inhibit TR. Among these molecules, compound 3 (2-(diethylamino)ethyl 4-((3-(4-nitrophenyl)-3-oxopropyl)amino) benzoate) was shown to inhibit TR in the micromolar range by binding to a unique cavity placed at the entrance of the NADPH-binding site, not present in the human homolog glutathione reductase (hGR) (Turcano et al. 2018).

The screening of our in house library of diaryl sulfides allowed us to identify a compound (RDS 777) able to inhibit TR in sub-micromolar range ($K_i = 0.25 \pm 0.18$ μM). The X-ray structure of *Li*TR-777 complex showed that the inhibitor is bound to both the trypanothione binding site and the NADPH-binding site. In particular, the monomer A binds three RDS 777 molecules, whereas the monomer B binds four RDS 777 molecules. RDS 777 *b* and *c* are bound in both monomers to the NADPH-binding site, whereas the RDS 777 *a* in the monomer A and *a* and *d* in monomer B are bound to the trypanothione-binding site. RDS 777 in position *a* interacts with the hydrophobic Val53 and Val58 and, furthermore, it is hydrogen bound to the residues more involved in the catalysis, namely His 461′, Glu466′, Cys57, Cys52 and Glu467′ (Saccoliti et al. 2017).

This binding mode of RDS 777 differs from that of the other diaryl sulfide derivatives reported in literature (Stump et al. 2008). Indeed, the diaryl sulfide derivative (3-({5-chloro-2-[(40-methylbiphenyl-4-yl)thio]phenyl} amino)-*N*-(3,4-dichlorobenzyl)-*N*,*N*-dimethylpropan-1-ammonium chloride)) modeled by Stump et al. accommodates in the trypanothione-binding cavity in the so-called "mepacrine"-binding site distant from the two catalytic cysteines. In the monomer B of LiTR-777 X-ray structure, an additional molecule of RDS 777 binds to the trypanothione-binding site (molecule *d*) close to the entrance of the trypanothione-binding site, establishes a stacking interaction with the pyrimidineamine moiety of the molecule *a* and is hydrogen bound to Glu467′.

In this paper, we report a structure-based anti-leishmaniasis drug design study: we have synthesized a series of diaryl compounds on the basis of the structure of RDS 777-TR complex and in particular of the sites *a* and *d*. Our studies allow the identification of a compound (RDS 562) able to inhibit TR, to kill the promastigote in the micromolar range and to reduce the intracellular concentration of reduced trypanothione. The compound specifically inhibits *Leishmania* TR, while it does not inhibit hGR. The inhibition assays demonstrate that RDS 562 inhibits TR by competing with trypanothione binding, and the docking experiments show the molecular basis of TR inhibition by the organic compound.

Materials and methods

Materials

Trypanothione disulfide (Bachem), NADPH (Panreac-Applichem), human glutathione reductase (Sigma-Aldrich) and oxidized glutathione (GSSG) (Sigma-Aldrich) were used for

the experiments. The *L. donovani* (BHU-1081) was obtained from Prof. Shyam Sundar, Banaras Hindu University, India, and cultivated M199 liquid media supplemented with 15% heat inactivated fetal bovine serum (FBS), 100 U/mL penicillin and 100 µg/ml streptomycin.

Chemistry: general

Melting points were determined with a Büchi 530 capillary apparatus and are uncorrected. Infrared (IR) spectra were recorded on a Perkin-Elmer Spectrum-One spectrophotometer. ^{1}H NMR spectra were recorded on a Bruker AC 400 spectrometer. Merck silica gel 60 F_{254} plates were used for analytical TLC. Developed plates were visualized by UV light. Column chromatography was performed on silica gel (Merck; 70–230 mesh) or aluminum oxide (Merck; 70–230 mesh). Compounds purities were always > 95% determined by high-pressure liquid chromatography (HPLC). HPLC analysis was carried out using Shimadzu LC-10AD VP and CTO-10AC VP. Column used was generally Suplex pKb-100 (250 mm × 4.6 mm, 5 µm). Microwave reactions were conducted using a CEM Discover system unit (CEM Corp., Matthews, NC, USA). The machine consists of a continuous focused microwave-power delivery system with operator selectable power output from 0 to 300 W. The temperature of the contents of the vessel was monitored using a calibrated infrared temperature control mounted under the reaction vessel. All experiments were performed using a stirring option whereby the contents of the vessel are stirred by means of a rotating magnetic plate located below the floor of the microwave cavity and a Teflon-coated magnetic stir bar in the vessel. Solvents were reagent grade and, when necessary, purified and dried by standard methods. Organic solutions were dried over anhydrous sodium sulfate (Merck). Concentration of solution after reactions and extractions involved the use of a rotary evaporator operating at reduced pressure of approximately 20 Torr. Analytical results agreed to within ± 0.40% of the theoretical values. Dimethylsulfoxide-d_6 99.9% (code 44139-2) and deuterochloroform 98.8% (code 41675-4) of isotopic purity (Aldrich) were used.

Intermediate 6-(*sec*-butoxy)-2-chloropyrimidin-4-amine and final products RDS 832, RDS 939 and RDS 1256 have been synthesized according to literature (Costi et al. 2000; Massa et al. 1994; Saccoliti et al. 2017).

Chemical, physical, and analytical data of the described compounds are previously reported (Costi et al. 2000; Massa et al. 1994).

General procedure (GP-A) for the synthesis of diaryl sulfide derivatives RDS 802, RDS 866

In a microwave vial, intermediate 6-(*sec*-butoxy)-2-chloropyrimidin-4-amine (0.25 M; 0.992 mmol) was dissolved in isopropanol (3.97 mL). To this solution, the proper benzenethiol (1.984 mmol) and DIPEA (1.984 mmol) were added. The vial was sealed and heated by microwave at 160 °C for 5 min. After cooling, the mixture was treated with water (3 mL) and extracted with ethyl acetate (3 × 3 mL). The organic extracts were collected, washed with brine (3 × 2 mL), dried over Na_2SO_4 and evaporated at reduced pressure. Raw materials were chromatographed on silica gel (*n*-hexane:acetone 5:1 as eluent) to furnish pure RDS 802 and RDS 866.

For each compound, new achieved yields (%) are reported.

General procedure (GP-B) for the synthesis of diaryl sulfide derivatives RDS 562, RDS 615 and RDS 771

The proper halopyrimidine (4.96 mmol) was added to a well-stirred solution of $Pd_2(dba)_3$ (49.6 µmol), DPPF (99.18 µmol), DIPEA (5.45 mmol) and the proper benzenethiol (4.96 mmol) in anhydrous DMF (7.5 mL) at room temperature. The reaction was stirred under reflux for the proper time and then cooled to room temperature, treated with water (50 mL) and extracted with chloroform (3 × 50 mL). The combined organic phases were washed with brine (5 × 20 mL), dried over Na_2SO_4 and evaporated at reduced pressure. The crude products were purified by column chromatography yielding pure derivatives RDS 562, RDS 615 and RDS 771. For each compound, yield (%), reaction time and chromatographic system are reported.

6-(*sec*-Butoxy)-2-((4-fluorophenyl)thio) pyrimidin-4-amine (RDS 802)

Compound RDS 802 was prepared from intermediate 6-(*sec*-butoxy)-2-chloropyrimidin-4-amine and 4-fluorothiophenol by means of GP-A. Yield 50%.

6-(*sec*-Butoxy)-2-((phenyl)thio)pyrimidin-4-amine (RDS 615)

Compound RDS 615 was prepared from intermediate 6-(*sec*-butoxy)-2-chloropyrimidin-4-amine and benzenethiol by means of GP-B. 55%; 6.5 h; SiO_2/*n*-hexane:acetone 5:1.

6-(*sec*-Butoxy)-2-((4-chlorophenyl)thio) pyrimidin-4-amine (RDS 771)

Compound RDS 771 was prepared from intermediate 6-(*sec*-butoxy)-2-chloropyrimidin-4-amine and 4-chlorothiophenol by means of GP-B. 69%; 6.5 h; SiO_2/*n*-hexane:acetone 5:1.

6-(*sec*-Butoxy)-2-((3-methoxyphenyl)thio) pyrimidin-4-amine (RDS 866)

Compound RDS 866 was prepared from intermediate 6-(*sec*-butoxy)-2-chloropyrimidin-4-amine and 3-methoxythiophenol by means of GP-A. Yield 79%.

2-Chloro-6-(phenylthio)pyrimidin-4-amine (RDS 562)

Compound RDS 562 was prepared from 4-amino-2,6-dichloropyrimidine and benzenethiol by means of GP-B. 7%; 5 h; Al_2O_3/$CHCl_3$:*n*-hexane 9:1.

Inhibition of promastigote growth

Promastigote (the extracellular stage of the *Leishmania* life cycle) growth inhibition was evaluated using *L. infantum* strain (MHOM/TN/80/IPT1). To estimate the 50% inhibitory concentration (IC_{50}), the MTT (3-[4.5-dimethylthiazol-2-yl]-2.5-diphenyltetrazolium bromide) micromethod (Sereno and Lemesre 1997) was used throughout the experiments with modification (Saccoliti et al. 2017).

Promastigotes were grown in Schneider's *Drosophila* medium (SIGMA) containing 10% fetal calf serum (FCS) (GIBCO-BRL) and 2% gentamicin (50 mg/L) (Sigma) at 22 °C.

Parasites were adjusted to 1×10^6 parasites/mL, and 200 µL of suspension was seeded in triplicate in 96-well flat bottom microplates and incubated with varying concentrations of compound. In a first screening 0.01, 0.1, 1, 10, 100 µM concentrations were used to evaluate the activity range of the drugs. In the second screening, the following drug concentrations were used to calculate the IC_{50}: 0.16, 0.32, 0.65, 1.31, 2.62, 5.25, 10.50, 21.00, 42.00, 84.00, 168.00, 320.00 µM.

Amphotericin B (IC_{50} 0.5 µM) (Euroclone) was used as control. Each experiment was done in triplicate for each drug concentration and two independent experiments were performed. After 72 h of incubation, 30 µL of MTT was added to each well and plates were further incubated for 2 h. The absorbance at 550 nm was measured with a 96-well scanner (DINEX Technologies, VA, USA). Anti-leishmanial activity per experimental point was expressed as mean percentage of inhibition with respect to vehicle treated parasites (0%). In addition, the promastigote vitality was followed by microscopic observation after 72 h. Data were analyzed and plotted by Prism (GraphPad, San Diego, USA).

Intracellular measurement of trypanothione concentration

The intracellular trypanothione ($T(SH)_2$) level was estimated in the procedure as reported previously (Bhattacharya et al. 2009; Mukhopadhyay et al. 1996; Saudagar et al. 2013; Wintner et al. 2010). In brief, *L. donovani* mid-log phase promastigotes (1×10^7 cells) cultures were incubated with IC_{50} dose of all synthesized drugs (Table 1) and RDS 777. Following incubation for 24 h, 1×10^7 cells were harvested by centrifugation (10,000 rpm, 10 min, 4 °C) and washed twice with PBS. Pellet was suspended in 100 µl buffer (50 mM HEPES at pH 8.0) containing 5 mM EDTA) taken in a dark tube, 100 µL of 2 mM monobromobimane (dissolve in ethanol) was added, and suspension was incubated at 70 °C for 3 min. Ice-cold 200 µL of 25% trichloroacetic acid were added to the suspension, which was incubated on ice for 20 min. The denatured protein and cell debris were removed by centrifugation. Acid-soluble thiols were separated by ion-paired, reverse phase HPLC on an ion-paired Ultrasphere C18 column with linear gradient of 0–90% methanol in 0.25% acetic acid (pH 3.5). Bimane-$T(SH)_2$ complex formation absorbance was taken at 254 nm, using a Dionex Ultimate 3000 instrument fitted with a Dionex RF-2000 absorbance detector. Absorbance of standard $T(SH)_2$–bimane complex formation was also measured at 254 nm. Experiments were performed in duplicate and the results are expressed as mean ± SD. Data were analyzed using Student's *t* test (one tailed) with the help of statistical software PRISM 5 (Graphpad software). The criterion for statistical significance between the groups was as follows: *p* value 0.05 was considered significant and marked as *, 0.01 as highly significant and marked as **, 0.001 as very highly significant and marked as ***.

Enzymatic assay

LiTR was expressed and purified as previously reported (Baiocco et al. 2009b). Enzymatic inhibition assays were carried out at 20 °C using a diode array Hewlett-Packard HP8452A spectrophotometer.

All the diaryl sulfide compounds were first tested at final concentration of 10 µM. The solution containing buffer (HEPES 50 mM, NaCl 40 mM at pH 7.4), TR 5 nM, TS_2 150 µM and inhibitor 10 µM was allowed to equilibrate for 2 min in a quartz cuvette. Assays were initiated by addition of NADPH 100 µM.

Table 1 IC_{50} values for each tested compound vs. *L. infantum* promastigotes. The data are expressed as mean ± standard error of two independent experiments performed in triplicate

Compound	IC50 (µM)
RDS 562	11 ± 2
RDS 615	31 ± 2
RDS 802	18 ± 1
RDS 832	15 ± 1
RDS 939	16 ± 1
RDS 1256	6.7 ± 0.2

Absorbance decrease was followed at 340 nm, indicating NADPH oxidation, and the percentage of inhibition was calculated by measuring the velocity of NADPH oxidation with respect to the experiment performed in absence of inhibitor. NADPH concentration was calculated using the molar extinction coefficient $\varepsilon = 6222/M/cm$.

As 10 μM RDS 562 displayed a percentage of inhibition higher than 30%, various conditions of inhibitor (0 μM, 6 μM, 8 μM, 10 μM) and substrate (50 μM, 100 μM, 150 μM) were tested to determine the inhibition constant, K_i of the compound through Dixon plot analysis.

Due to solubility/aggregation problems, determination of RDS 562 inhibition was not possible at higher concentrations. Every experiment was carried out in triplicate.

In order to verify selectivity, RDS 562 was tested on glutathione reductase, the homologous human protein of TR, in the same conditions of the screening assay: GR 5 nM, GSSG 150 μM, RDS 562 (0, 8, 10, 12, 20 μM) in buffer 20 mM HEPES, 40 mM NaCl pH 7.4.

The linear regression analyses were performed with Microsoft Excel (version 2013).

Docking experiments

The TR structure in complex with RDS 777 was retrieved from PDB (Id: 5ebk) and prepared by deleting ions, water molecules and crystallization additives and by adding hydrogen atoms. To be compatible with physiological pH, Asp, Glu, Lys and Arg residues were considered ionized while His and Cys residues neutral by default. The protein structure was then minimized by fixing the backbone atoms to preserve the resolved folding. After deleting the bound inhibitors, the so refined TR structure underwent docking simulations. The conformational profile of the considered ligands was explored by Monte Carlo procedures as implemented in the VEGA software (Pedretti et al. 2002), which generates 1000 minimized conformers for each ligand. The so-derived lowest energy structure underwent docking simulations after a final optimization by PM7-based semi-empirical calculations (Stewart 2013). Docking simulations were performed by PLANTS (Korb et al. 2009) and attention was focused on three possible binding sites as derived by the resolved structure: the first (named site *a*) corresponds to the resolved pose in the catalytic site, the second (site *d*) is adjacent to site *a* and slightly more external towards the entrance of the catalytic pocket while the third binding site (site *c*) is rather superficial at the entrance of the NADPH-binding site. Hence, docking searches were focused within a 15 Å radius sphere around the resolved RDS 777 pose corresponding to site *a* as well as within a 10 Å radius sphere around the resolved RDS 777 pose corresponding to site *c*. Notice that the sphere size for the first search was selected to encompass both binding sites *a* and *d* and the simulations were repeated with and without a penalty (equal to − 3.0 kcal/mol) to constraint the ligands within the site *a* to better evaluate the mutual preference between the two binding sites. For each simulated inhibitor, ten poses were generated and ranked by the ChemPLP scoring function with a speed equal to 1. The poses were then minimized and rescored by using ReScore+ (Vistoli et al. 2017).

Results

Synthesis of diaryl sulfide compounds

Compounds RDS 562, RDS 615, RDS 802, RDS 832, RDS 939 and RDS 1256 have been synthesized according to Scheme 1.

The synthesis of such derivatives has been already reported in literature by our research group (Costi et al. 2000); however, in the current work some steps of the previously described synthetic pathway have been changed for both safety and saving time reasons. In particular, all the synthetic steps involving the use of benzenethiol reagents in nucleophilic aromatic substitution have been properly modified. The originally reported synthetic route was based on the use of in situ prepared potassium thiophenolates, which are well-known dangerous and difficult to handle reagents. Moreover, in general, reactions involving such reactants usually require long time to achieve the product. For instance, despite its notable yield, nucleophilic aromatic substitution reaction leading to reference compound RDS 777 was reported to take place in 1 week (Costi et al. 2000).

Thus, according to the synthetic approach already applied for the re-synthesis of RDS 777 (Saccoliti et al. 2017), the introduction of thiophenol groups on the central pyrimidine core was achieved through alternative synthetic routes. In particular, microwave-assisted or Pd-catalyzed batch reactions have been employed, in order to overcome the aforementioned limits of the previously reported pathway.

The commercially available product 4-amino-2,6-dichloropyrimidine underwent a nucleophilic aromatic substitution in the presence of sodium *sec*-butoxide, which was in situ prepared from anhydrous *sec*-butanol and metallic sodium, as previously reported (Costi et al. 2000; Massa et al. 1994; Saccoliti et al. 2017).

The reaction was performed in the same solvent for 4 h, leading to intermediate 6-(*sec*-butoxy)-2-chloropyrimidin-4-amine as main product.

Applying the recently reported procedure employed for the re-synthesis of RDS 777 (Saccoliti et al. 2017), diaryl sulfide derivatives RDS 562, RDS 615 and RDS 771 have been synthesized through a modified Buchwald–Hartwig C-S cross coupling reaction by using the proper thiophenol in the presence of $Pd(dba)_3$, DPPF and DIPEA in anhydrous

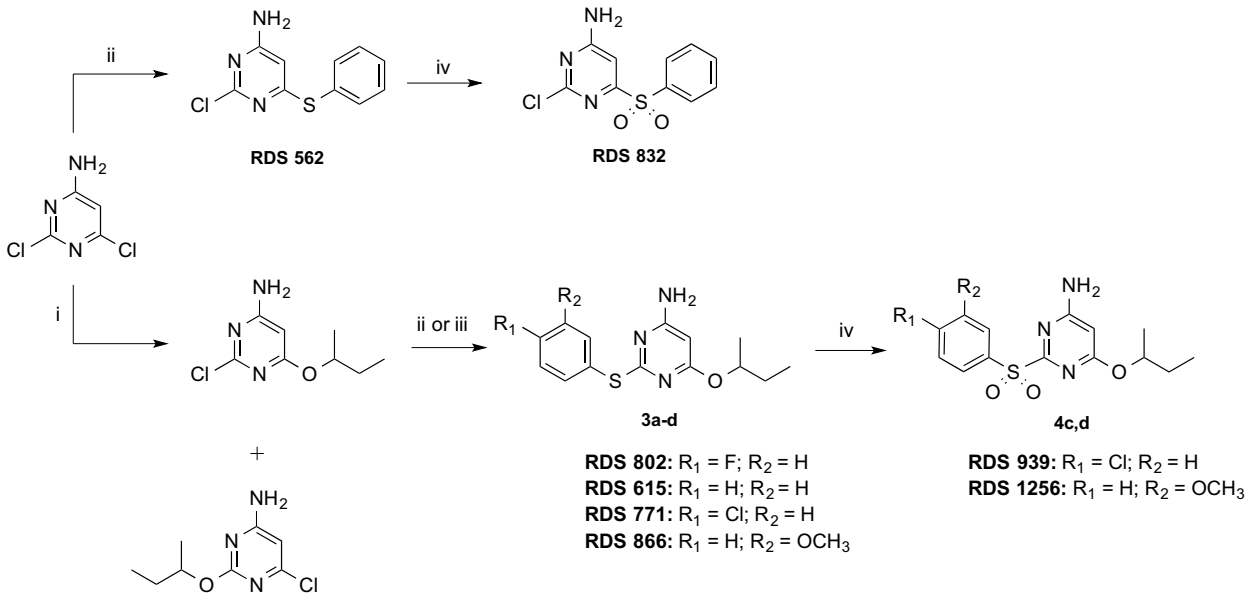

Reagents and conditions: (i) *sec*-$BuOH_a$, Na, reflux, 4h, Ar, 60%; (ii) proper thiophenol, $Pd_2(dba)_3$, DPPF, DIPEA, DMF_a, reflux, 5-6,5h, Ar, 7-69%; (iii) proper thiophenol, DIPEA, iPrOH 0.25M, MW, 160°C, 5 min, 50-79%; (iv) H_2O_2 30%, AcOH gl., 60°C, 4-7.5 h, 23-87%.

Scheme 1 Synthesis of compounds RDS 562, RDS 615, RDS 802, RDS 832, RDS 939 and RDS 1256

DMF. Alternatively, a previously reported microwave-assisted procedure (Luo et al. 2002) was applied for the synthesis of thioethers RDS 802 and RDS 866. Notably, such reaction, which was performed in the presence of the proper thiophenol and DIPEA in isopropanol 0.25 M, took place in only 5 min at 160 °C, yielding the products in good yields.

Sulfone derivatives RDS 832, RDS 939 and RDS 1256 have been synthesized from the corresponding thioether intermediates RDS 562, RDS 771 and RDS 866 in the presence of hydrogen peroxide 30% in glacial acetic acid at 60 °C, according to literature (Costi et al. 2000).

Activity against *L. infantum* promastigote

Diaryl sulfides induced a dose-dependent anti-proliferative effect on *L. infantum* promastigotes that was observed by both MTT enzymatic assay and microscopic observations.

The results of the first screening showed that all compounds induced 90% promastigote mortality at a concentration around 100 µM. At this concentration, RDS compounds induced mortality observed by microscopy, i.e., the parasites appeared as rounded, aflagellated and vacuolated cells, arranged in clusters along the edges of the microplate well. At 'sublethal' concentrations (between 1 and 100 µM), a dose-dependent leishmanistatic activity was observed. Indeed, the parasites showed motility inhibition (with a reduced flagellum) and body swelling, not present in control cells. At submicromolar concentrations (below 0.3 µM), no changes in promastigote morphology, motility and growth were observed with respect to control cells. Table 1 reports the IC_{50} values of the tested compounds, showing that all synthesized compounds are able to kill promastigote in micromolar range. RDS 562, the compound more active against trypanothione metabolism (see below), at dose 168 µM, induced 100% promastigote mortality, whereas at 'sublethal' concentrations, ranging from 84.00 to 0.65 µM, showed a dose-dependent leishmanistatic activity. Lower concentrations, $\leq$0.3 µM, did not affect promastigote growth (Fig. 2).

Intracellular measurement of trypanothione concentration

The promastigote cells treated with IC_{50} dose of all drugs for 24 h showed significant changes in the levels of intracellular $T(SH)_2$. Interestingly all the RDS compounds with the exception of RDS 777 and RDS 562 display an increase in $T(SH)_2$ concentration in the cell (data not shown) indicating that TR is not the main target for these compounds.

On the contrary a decrease of 33.15% of $T(SH)_2$ was observed in RDS 562- and of 38.5% in RDS 777-treated cells, as compared to untreated control cells (Fig. 3) indicating that these compounds affect the trypanothione metabolism and act preferentially by inhibiting TR. As reported in Fig. 3, the inhibitor concentrations used for the experiments correspond to the IC_{50} values of RDS 777 and RDS 562,

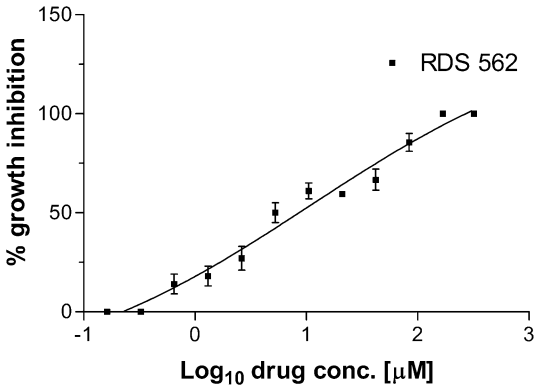

Fig. 2 Growth inhibition induced by RDS 562. % of growth inhibition calculated on *L. infantum* promastigote stage after treatment with various concentrations of RDS 562. The data are expressed as mean ± standard error of two independent experiments performed in triplicate

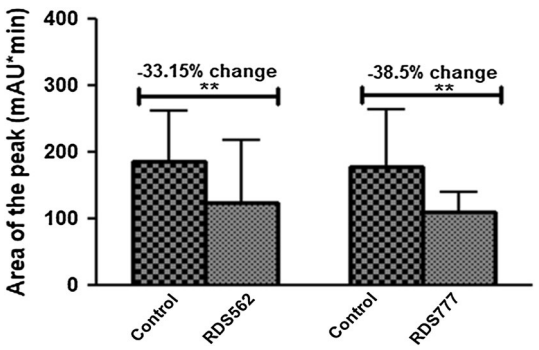

Fig. 3 Measurement of intracellular thiol level in both untreated *Leishmania donovani* (control) and drug (RDS 562 and RDS 777) treated *Leishmania donovani* promastigotes. Results are expressed as average value of area of the peak of two independent experiments ($n=2$). Percentage changes in the case of two samples (RDS777 and RDS562) were calculated considering average peak value of control as 100. Results are expressed as mean ± SD. Data were analyzed using Student's *t* test (one tailed) with the help of statistical software PRISM 5 (Graphpad software). The criterion for statistical significance between the groups was as follows: *p* value, 0.05 was considered significant and marked as *, 0.01 as highly significant and marked as **, 0.001 as very highly significant and marked as ***

respectively. Thus, since the concentration of RDS 777 used in the experiments (29.43 μM) is three times higher than the concentration of RDS 562 used in the experiment (11 μM), it follows that RDS 562 results to be more active than RDS 777 on the trypanothione metabolism.

Enzymatic assays

Kinetic studies were performed on RDS 562 endowed with the highest activity against the promastigote forms of *L. donovani* and vs. trypanothione levels. Steady state kinetic experiments were carried out at various concentrations of TS_2 and RDS 562, while fixed TR and NADPH concentrations (5 nM and 100 μM, respectively) were maintained. After starting the reaction by the addition of NADPH, the absorbance decrease at 340 nm, indicative of NADPH oxidation, was measured (Baiocco et al. 2009a). As shown in Fig. 4a, RDS 562 inhibited the binding of TS_2 to TR. Each line in the Dixon plot represents linear regression analysis of reciprocal average fitted rates of TS_2 reduction for different substrate concentrations, as a function of inhibitor concentration. The K_M and k_{cat} of TR used for the K_i calculation were 23.0 ± 1.0 μM and 11.4 ± 0.3 s^{-1}, respectively. The value of K_i calculated from the Dixon plot analysis was 12.0 ± 1.0 μM, higher than that of Sb(III) (1.5 μM) (Baiocco et al. 2009a). The Lineweaver–Burk plot, representing linear regression analysis of reciprocal average fitted rates of TS_2 reduction for different inhibitor concentrations as a function of substrate concentrations, clearly demonstrates that RDS 562 is a competitive inhibitor. Indeed, as shown in Fig. 4b, V_{max} does not change whereas the apparent K_M increases as a function of the inhibitor concentration increase (Fig. 4b).

RDS 562 was tested also on hGR and, as shown in Fig. 4c, it is not effective on the human homolog of TR (Fig. 4c).

Docking experiments

The docking experiments have been performed using all the synthesized compounds, but we focalized our discussion on RDS 562 which is the only one able to reduce the trypanothione concentration in cells and therefore acting preferentially on the trypanothione reductase enzyme.

As explained under methods, the sites *a* and *d* are adjacent and partly overlapped and therefore a single docking simulation can comprise both sites, thus evaluating the relative preference of each ligand for them. A bird's eye analysis of all docking results and of relative scoring functions reveals that all simulating ligands are properly accommodated within the site *a* only when applying the constraint penalty. When docking search is left unconstrained, the ligands markedly prefer to engage the site *d*. The clear preference is reflected into all computed docking scores which shows better values when considering the unconstrained docking simulation thus suggesting that the binding to site *d* allows the ligand to stabilize stronger interactions compared to site *a*. For example, the primary score ChemPLP reveals a decrease average of 4.3 kcal/mol shifting from −61.9 to −57.6 kcal/mol. Notably, the comparison of docking scores between site *a* and *d* (Table 2) reveals that the tighter contacts involve both polar and hydrophobic interactions thus suggesting that the ligand polarity should not significantly influence the preference between binding sites. Figure 5 compares the best pose of RDS 562 within site *a* and site *d*. In the site *a* (see Fig. 5a), RDS 562 is seen to assume a flipped pose

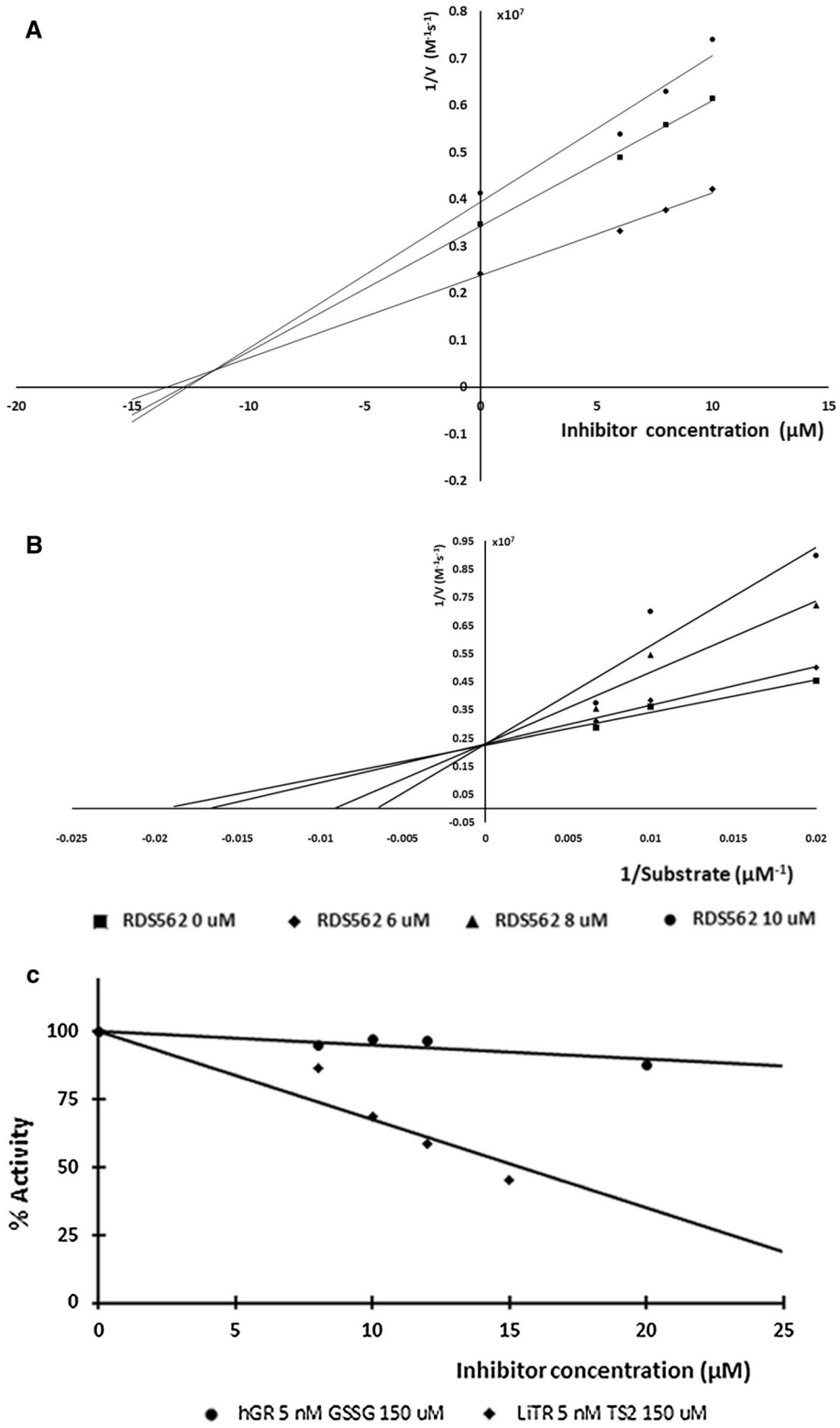

Fig. 4 Inhibition assays. **a** Dixon plot of *Li*TR inhibition with RDS 562. Linear regression was performed using four inhibitor concentrations (0 µM RDS 562; 6 µM RDS 562; 8 µM RDS 562; 10 µM RDS 562) and three TS_2 concentrations (50 µM TS_2, filled circles, $R^2 = 0.9386$; 100 µM, filled squares TS_2, $R^2 = 0.9941$; 150 µM TS_2, filled diamonds, $R^2 = 0.9875$). Each point represent the mean of three experiments; the assay was performed in buffer Hepes 20 mM, 40 mM NaCl pH 7,4, in presence of 5 nM LiTR, and 100 µM NADPH. **b** Lineweaver–Burk plot. RDS 562 inhibits LiTR in a competitive fashion; linear regression was performed with four inhibitor concentrations (0 µM RDS 562, filled squares, $R^2 = 0.9502$; 6 µM RDS 562, filled diamonds, $R^2 = 0.9746$; 8 µM RDS 562, filled triangles, $R^2 = 0.9103$; 10 µM RDS 562, filled circles, $R^2 = 0.8356$). Each line is the mean of three experiments; the assay was performed in buffer Hepes 20 mM, 40 mM NaCl pH 7,4, in presence of 5 nM LiTR, 50 µM, 100 µM and 150 µM of TS_2 and 100 µM NADPH. **c** Inhibition assays on TR and GR. RDS 562 is not active against hGR ($IC_{50} > 100$ µM) (filled circles). On the contrary, LiTR activity decreases as a function of RDS 562 concentrations (filled diamonds). Both the experiments were performed in buffer Hepes 20 mM, 40 mM NaCl pH 7.4, in presence of 5 nM enzyme, 150 µM of TS_2 and 100 µM of NADPH. Each line is expression of three independent experiments (RDS 562 vs hGR $R^2 = 0.8017$; RDS 562 vs LiTR $R^2 = 0.8930$)

compared to the corresponding resolved RDS 777 pose by which the 4-aminopyrimidine ring elicits a set of H-bonds involving Ser14, Tyr110 and Thr335 of chain A, while the phenyl ring approaches the chain B by contacting His461′, Pro462′ and Glu466′. Thus and similarly to what was seen for RDS 777, the binding site *a* comprises both subunits even though with a different involvement. Indeed, while for RDS 777 the key polar contacts were stabilized by residues

Table 2 Representative docking scores for the three considered binding sites for RDS 562

RDS 562	LJ_CHARMM (kcal/mol)	Elect_DD (kcal/mol)	CHEMPLP (kcal/mol)
Site *d*	− 25.51	− 6.95	− 9.84
Site *a*	− 21.63	− 4.03	− 53.63
Site *c*	− 22.83	− 9.84	− 54.77

The primary ChemPLP score is computed by PLANTS and encodes for both ionic and non-polar contacts while LJ_CHARMM and Elec_DD are computed by VEGA and encode for the van der Waals contacts as calculated by the Lennard-Jones term of the CHARMM force field and the ionic interactions by using a distance dependent dielectric function, respectively (all scores are expressed in kcal/mol)

of the chain B, and the chain A takes part only by hydrophobic contacts, the key H-bonds of RDS 562 involve the chain A, while the chain B elicits almost only hydrophobic contacts. Despite the described differences, both ligands (RDS 777 and RDS 562) emphasize the pivotal role of His461′, which stabilizes π–π stacking with both aromatic rings plus a weak H-bond with the thioether linker. Figure 5b shows the putative complex of RDS 562 within the binding site *d*, which is almost completely lined by residues of the chain B. In detail and similarly to the corresponding resolved pose of RDS 777, RDS 562 is seen to elicit H-bonds which involve the 4-aminopyrimidine ring with Glu466′ and Glu467′. The pyrimidine ring also stabilizes a clear π–π stacking interaction with Phe396′, while the phenyl ring is mostly engaged in hydrophobic contacts which involve Pro398′, Leu399′ and Pro462′. The only involvement of the chain A is represented by Lys61, which approaches the ligand phenyl ring stabilizing charge transfer interactions. The analysis of the docking results for the other two compounds containing a thioether linker reveals binding modes rather similar to that above described for both binding sites *a* and *d*. A slightly more heterogeneous behavior is shown by the three derivatives including an oxidized sulphonyl linker. In detail RDS 832 is able to retain similar poses both in the site *a* where the sulphonyl group elicits a strong H-bond with His461′ and in the site *d* where the sulphonyl approaches Lys61. The increase of the steric hindrance in RDS 939 has a rather destabilizing effect especially for the binding site *a* and indeed few computed RDS 939 poses appear suitably arranged there. The site *d* appears to be more able to accommodate these sulphonyl derivatives with an increased relevance of the polar contacts elicited by Lys61 as mentioned above. On these grounds, one may understand why the further increase of size and polarity render the most active RDS 1256 a sort of exception since it is unable to engage the site *a* even

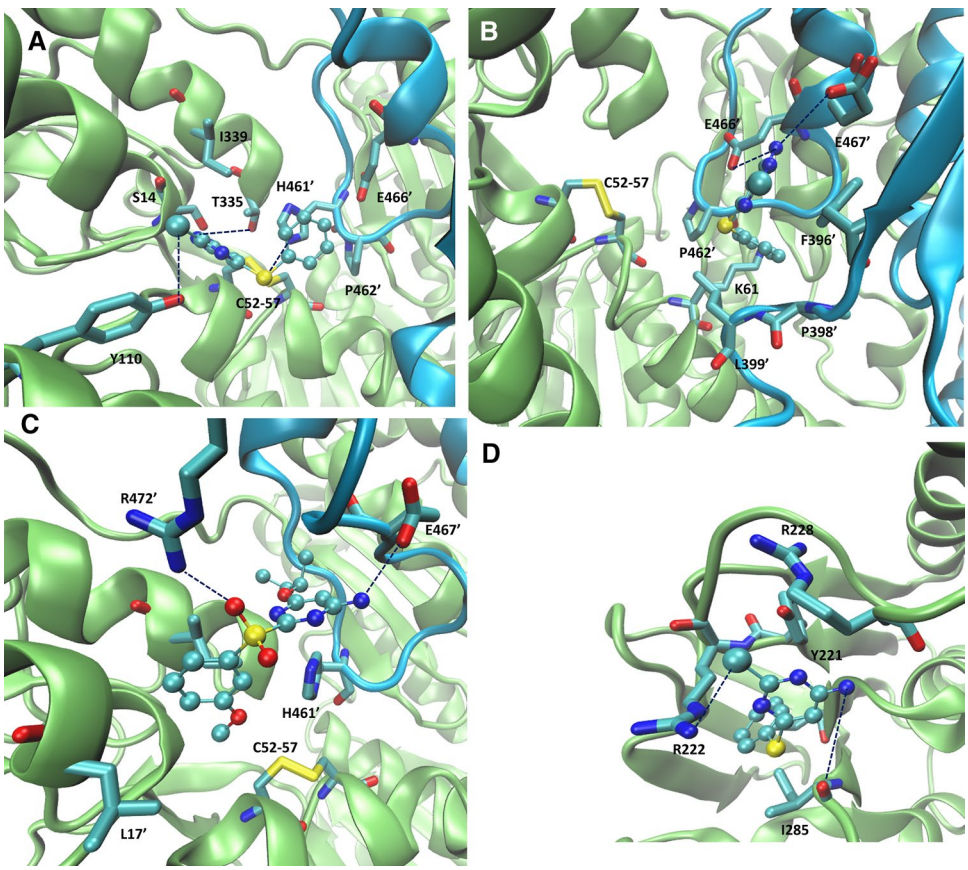

Fig. 5 Docking results. Main interactions stabilizing the putative complexes of RDS 562 within the binding site *a* (**a**), site *d* (**b**) and site *c* (**d**). Main interactions stabilizing RDS 1256 in the binding site *d* (**c**)

when performing constrained docking simulations and in both docking runs it occupies the binding site *d* assuming a slightly extended pose by which its sulphonyl group is able to contacts Arg472′ while the pyrimidine ring maintains its interactions with Glu466′ and Glu467′ (see Fig. 5c).

Finally, Fig. 5d shows the best putative complex as computed for RDS 562 within the binding site *c* where it approaches Arg222 and Arg228 with which it can stabilize both H-bonds and charge transfer interactions. The computed complex appears to be further stabilized by π–π stacking involving Tyr221 which is also engaged by a halogen bond with chlorine atom plus hydrophobic contacts with Ile285 and Val194. All simulated compounds show similar interaction patterns with the sulphonyl derivatives which elicits strong polar interactions with the surrounding arginine residues.

The analysis of the computed docking scores for the site *c* reveals, on average, worst values compared to both binding site *a* and *d*. For example, the primary score ChemPLP shows a decrease average of 8 kcal/mol when comparing site *d* and *c* and of 3.7 kcal/mol between site *a* and site *c*. The general worsening of the docking scores for the site *c* is clearly explainable when considering that it is on the protein surface and thus the ligands are not completely surrounded by interacting residues. Considering the described interactions, it comes as no surprise that the only docking scores which shows better values for the site *c* is that describing the ionic contacts based on a distance dependent dielectric constant.

Discussion

Leishmania parasites rely on a unique and essential thiol-based redox metabolism based on trypanothione (Comini and Flohé 2013; Krauth-Siegel and Comini 2008; Oza et al. 2005), while a system of redox homeostasis based on catalase and glutathione reductase is absent in the parasite. Therefore, inhibition of the enzymes of the trypanothione pathway is one of the most attractive options for anti-kinetoplastid drug discovery.

On the basis of the crystal structure of the diaryl sulfide RDS 777 in complex with *Li*TR, we synthesized a series of diaryl sulfides able to inhibit the *Leishmania* growth in the promastigote stage displaying a IC_{50} ranging from 6 to 30 μM (Table 1). Among them RDS 1256 and RDS 562 are inhibitors of *Leishmania* parasite growth more potent than RDS 777 but only RDS 562 besides RDS 777 is able to significantly decrease the amount of reduced trypanothione in the *Leishmania donovani* promastigotes. As shown by the inhibition assays, RDS 562 is able to selectively inhibit the trypanothione reductase, displaying an inhibition constant of 12.0 ± 1.0 μM, while it does not inhibit the human homologous GR. The value of K_i calculated from the Dixon plot analysis for RDS 562 is an order of magnitude higher than that calculated for RDS 777 (0.25 μM) and more than six times higher than that of Sb(III) (1.5 μM), the active form of antimonials, the most used drug against Leishmaniasis, calculated by Baiocco et al. (2009a) and about two times higher than that of compound 1 (4.6 ± 2.5 μM) (Baiocco et al. 2013).

The docking studies performed on TR with RDS 562 starting from the binding sites of RDS 777 on the complex structure TR-777 shows that whereas this compounds preferentially binds to the so-called site *a*, RDS 562 binds preferentially to site *d*. Indeed, the structural analysis performed on the complex LiTR-777 show that RDS 777 binds to both the TR subunit A and B in the site *a*, whereas only in the B subunit binds to the site *d* with an occupancy of 0.8 indicating a higher affinity of RDS 777 for the *a* site; on the contrary when RDS 562 docking search is performed on TR unconstrained, the ligand markedly prefers to engage the site *d*. The clear preference is reflected into all computed docking scores which show better values when considering the unconstrained docking simulation thus suggesting that the binding site *d* allows the ligand to stabilize stronger interactions compared to site *a* (Table 2, Fig. 5).

The data presented in this paper show that we succeeded to find a new diaryl sulfide compound able to kill Leishmania parasites with a higher efficiency with respect to RDS 777. Indeed the IC_{50} of RDS 777 is 29 ± 1 μM, whereas the IC_{50} of RDS 562 is 11 ± 2 μM. Our data show that RDS 562 target specifically the trypanothione metabolism by decreasing its concentration in the cell through TR inhibition.

Even if the ability to inhibit TR of RDS 562 is an order of magnitude lower than that of RDS 777, the docking studies show that whereas RDS 777 binds to four different TR sites (*a–d*), RDS 562 is able to bind preferentially to the site *d* in the trypanothione binding cavity whereas its affinity for the other binding sites is negligible. More importantly, RDS 562 is able to reduce the intracellular reduced trypanothione concentration of about 33% when added to the medium at a concentration of 11 μM ($= IC_{50}$), whereas RDS 777 is able to reduce the reduced trypanothione concentration of 38% when added to the medium at a concentration three times higher (29 μM).

In conclusion, among diaryl sulfides, RDS 562 which is able to kill *Leishmania* parasites and to decrease trypanothione concentration in the promastigote stage, by competing with trypanothione binding, without off-target effects, can represent a new promising compound to find new drugs against visceral leishmaniasis; in addition, since the residues lining the trypanothione binding cavity of TR are strictly conserved, it could also represent a promising molecule for the treatment of other related neglected diseases caused by Trypanosomatids such as Chagas' disease, caused

by *Trypanosoma cruzi*, and the African sleeping sickness, caused by *T. brucei*, diseases against which no effective and safe therapies are available.

Acknowledgements We gratefully acknowledge CNCCS CNR (National Collection of Chemical Compounds and Screening Center 2018) to AI and MIUR PRIN 20154JRJPP to GC which supported the experiments reported in these studies. This paper is dedicated to the memory of our friend and colleague Prof. Emilia Chiancone, passed away sadly in December 2018.

Compliance with ethical standards

Conflict of interest The authors declare that they have no conflict of interest.

Research involving human participants and/or animals This article does not contain any studies with human participants or animals performed by any of the authors.

Informed consent Informed consent was obtained from all individual participants included in the study.

References

Bailey S, Smith K, Fairlamb AH, Hunter WN (1993) Substrate interactions between trypanothione reductase and *N*1-glutathionylspermidine disulphide at 0.28-nm resolution. Eur J Biochem FEBS 213:67–75

Baiocco P, Colotti G, Franceschini S, Ilari A (2009a) Molecular basis of antimony treatment in leishmaniasis. J Med Chem 52:2603–2612. https://doi.org/10.1021/jm900185q

Baiocco P, Franceschini S, Ilari A, Colotti G (2009b) Trypanothione reductase from *Leishmania infantum*: cloning, expression, purification, crystallization and preliminary X-ray data analysis. Protein Pept Lett 16:196–200

Baiocco P, Ilari A, Ceci P, Orsini S, Gramiccia M, Di Muccio T, Colotti G (2011) Inhibitory effect of silver nanoparticles on trypanothione reductase activity and *Leishmania infantum* proliferation. ACS Med Chem Lett 2:230–233. https://doi.org/10.1021/ml1002629

Baiocco P et al (2013) Inhibition of *Leishmania infantum* trypanothione reductase by azole-based compounds: a comparative analysis with its physiological substrate by X-ray crystallography. ChemMedChem 8:1175–1183. https://doi.org/10.1002/cmdc.201300176

Bhattacharya A, Biswas A, Das PK (2009) Role of a differentially expressed cAMP phosphodiesterase in regulating the induction of resistance against oxidative damage in *Leishmania donovani*. Free Radic Biol Med 47:1494–1506. https://doi.org/10.1016/j.freeradbiomed.2009.08.025

Burza S, Croft SL, Boelaert M (2018) Leishmaniasis. Lancet 392:951–970. https://doi.org/10.1016/S0140-6736(18)31204-2

Colotti G, Ilari A (2011) Polyamine metabolism in Leishmania: from arginine to trypanothione. Amino Acids 40:269–285. https://doi.org/10.1007/s00726-010-0630-3

Colotti G, Baiocco P, Fiorillo A, Boffi A, Poser E, Chiaro FD, Ilari A (2013a) Structural insights into the enzymes of the trypanothione pathway: targets for antileishmaniasis drugs. Future Med Chem 5:1861–1875. https://doi.org/10.4155/fmc.13.146

Colotti G et al (2013b) Metal-based compounds as prospective antileishmanial agents: inhibition of trypanothione reductase by selected gold complexes. ChemMedChem 8:1634–1637. https://doi.org/10.1002/cmdc.201300276

Colotti G, Fiorillo A, Ilari A (2018) Metal- and metalloid-containing drugs for the treatment of trypanosomatid diseases. Front Biosci (Landmark Ed) 23:954–966

Comini MA, Flohé L (2013) Trypanothione-based redox metabolism of trypanosomatids. In: Jäger T, Koch O, Flohé L (eds) Trypanosomatid diseases. Wiley-VCH Verlag GmbH & Co. KGaA, Hoboken, pp 167–199. https://doi.org/10.1002/9783527670383.ch9

Costi R et al (2000) Structure-activity relationship studies on potential non-nucleoside DABO-like inhibitors of HIV-1 reverse transcriptase. Antivir Chem Chemother 11:117–133. https://doi.org/10.1177/095632020001100204

Desjeux P (2004) Leishmaniasis: current situation and new perspectives. Comp Immunol Microbiol Infect Dis 27:305–318. https://doi.org/10.1016/j.cimid.2004.03.004

Dixon MJ, Maurer RI, Biggi C, Oyarzabal J, Essex JW, Bradley M (2005) Mechanism and structure–activity relationships of norspermidine-based peptidic inhibitors of trypanothione reductase. Bioorg Med Chem 13:4513–4526. https://doi.org/10.1016/j.bmc.2005.04.039

Dumas C et al (1997) Disruption of the trypanothione reductase gene of Leishmania decreases its ability to survive oxidative stress in macrophages. EMBO J 16:2590–2598. https://doi.org/10.1093/emboj/16.10.2590

Hamilton CJ, Saravanamuthu A, Eggleston IM, Fairlamb AH (2003) Ellman's-reagent-mediated regeneration of trypanothione in situ: substrate-economical microplate and time-dependent inhibition assays for trypanothione reductase. Biochem J 369:529–537. https://doi.org/10.1042/BJ20021298

Hamilton CJ, Saravanamuthu A, Poupat C, Fairlamb AH, Eggleston IM (2006) Time-dependent inhibitors of trypanothione reductase: analogues of the spermidine alkaloid lunarine and related natural products. Bioorg Med Chem 14:2266–2278. https://doi.org/10.1016/j.bmc.2005.11.004

Holloway GA et al (2007) Discovery of 2-iminobenzimidazoles as a new class of trypanothione reductase inhibitor by high-throughput screening. Bioorg Med Chem Lett 17:1422–1427. https://doi.org/10.1016/j.bmcl.2006.11.090

Hotez PJ, Savioli L, Fenwick A (2012) Neglected tropical diseases of the Middle East and North Africa: review of their prevalence, distribution, and opportunities for control. PLoS Negl Trop Dis 6:e1475. https://doi.org/10.1371/journal.pntd.0001475

Ilari A et al (2012) A gold-containing drug against parasitic polyamine metabolism: the X-ray structure of trypanothione reductase from *Leishmania infantum* in complex with auranofin reveals a dual mechanism of enzyme inhibition. Amino Acids 42:803–811. https://doi.org/10.1007/s00726-011-0997-9

Ilari A, Fiorillo A, Baiocco P, Poser E, Angiulli G, Colotti G (2015) Targeting polyamine metabolism for finding new drugs against leishmaniasis: a review. Mini Rev Med Chem 15:243–252

Ilari A, Fiorillo A, Genovese I, Colotti G (2017) Polyamine–trypanothione pathway: an update. Future Med Chem 9:61–77. https://doi.org/10.4155/fmc-2016-0180

Ilari A, Genovese I, Fiorillo F, Battista T, De Ionna I, Fiorillo A, Colotti G (2018) Toward a drug against all kinetoplastids: from leishbox to specific and potent trypanothione reductase inhibitors. Mol Pharm 15:3069–3078. https://doi.org/10.1021/acs.molpharmaceut.8b00185

Korb O, Stutzle T, Exner TE (2009) Empirical scoring functions for advanced protein-ligand docking with Plants. J Chem Inf Model 49:84–96. https://doi.org/10.1021/ci800298z

Krauth-Siegel RL, Comini MA (2008) Redox control in trypanosomatids, parasitic protozoa with trypanothione-based thiol metabolism. Biochim Biophys Acta 1780:1236–1248. https://doi.org/10.1016/j.bbagen.2008.03.006

Luo GL, Chen L, Poindexter GS (2002) Microwave-assisted synthesis of aminopyrimidines. Tetrahedron Lett 43:5739–5742. https://doi.org/10.1016/S0040-4039(02)01190-5

Martyn DC, Jones DC, Fairlamb AH, Clardy J (2007) High-throughput screening affords novel and selective trypanothione reductase inhibitors with anti-trypanosomal activity. Bioorg Med Chem Lett 17:1280–1283. https://doi.org/10.1016/j.bmcl.2006.12.016

Massa SDS, Costi R, Artico R, Loi M, Doa AG, Scano M, La Colla P (1994) Synthesis of novel HEPT analogues with anti-HIV-1 activity. Med Chem Res 4:554–562

Mukhopadhyay R, Kapoor P, Madhubala R (1996) Antileishmanial effect of a potent *S*-adenosylmethionine decarboxylase inhibitor: CGP 40215A. Pharmacol Res 33:67–70. https://doi.org/10.1006/phrs.1996.0011

Oza SL, Shaw MP, Wyllie S, Fairlamb AH (2005) Trypanothione biosynthesis in Leishmania major. Mol biochem Parasitol 139:107–116. https://doi.org/10.1016/j.molbiopara.2004.10.004

Patterson S et al (2011) Dihydroquinazolines as a novel class of Trypanosoma brucei trypanothione reductase inhibitors: discovery, synthesis, and characterization of their binding mode by protein crystallography. J Med Chem 54:6514–6530. https://doi.org/10.1021/jm200312v

Pedretti A, Villa L, Vistoli G (2002) VEGA: a versatile program to convert, handle and visualize molecular structure on Windows-based PCs. J Mol Graph Model 21:47–49

Saccoliti F et al (2017) Inhibition of *Leishmania infantum* trypanothione reductase by diaryl sulfide derivatives. J Enzyme Inhib Med Chem 32:304–310. https://doi.org/10.1080/14756366.2016.1250755

Saravanamuthu A, Vickers TJ, Bond CS, Peterson MR, Hunter WN, Fairlamb AH (2004) Two interacting binding sites for quinacrine derivatives in the active site of trypanothione reductase: a template for drug design. J Biol Chem 279:29493–29500. https://doi.org/10.1074/jbc.M403187200

Saudagar P, Saha P, Saikia AK, Dubey VK (2013) Molecular mechanism underlying antileishmanial effect of oxabicyclo[3.3.1] nonanones: inhibition of key redox enzymes of the pathogen. Eur J Pharm Biopharm 85:569–577. https://doi.org/10.1016/j.ejpb.2013.08.014

Sereno D, Lemesre JL (1997) Use of an enzymatic micromethod to quantify amastigote stage of *Leishmania amazonensis* in vitro. Parasitol Res 83:401–403

Spinks D et al (2009) Investigation of trypanothione reductase as a drug target in *Trypanosoma brucei*. ChemMedChem 4:2060–2069. https://doi.org/10.1002/cmdc.200900262

Stewart JJ (2013) Optimization of parameters for semiempirical methods VI: more modifications to the NDDO approximations and re-optimization of parameters. J Mol Model 19:1–32. https://doi.org/10.1007/s00894-012-1667-x

Stump B, Eberle C, Kaiser M, Brun R, Krauth-Siegel RL, Diederich F (2008) Diaryl sulfide-based inhibitors of trypanothione reductase: inhibition potency, revised binding mode and antiprotozoal activities. Org Biomol Chem 6:3935–3947. https://doi.org/10.1039/b806371k

Turcano L et al (2018) Identification and binding mode of a novel Leishmania Trypanothione reductase inhibitor from high throughput screening. PLoS Negl Trop Dis 12:e0006969. https://doi.org/10.1371/journal.pntd.0006969

Vistoli G, Mazzolari A, Testa B, Pedretti A (2017) Binding space concept: a new approach to enhance the reliability of docking scores and its application to predicting butyrylcholinesterase hydrolytic activity. J Chem Inf Model 57:1691–1702. https://doi.org/10.1021/acs.jcim.7b00121

Wintner EA et al (2010) A monobromobimane-based assay to measure the pharmacokinetic profile of reactive sulphide species in blood. Br J Pharmacol 160:941–957. https://doi.org/10.1111/j.1476-5381.2010.00704.x

Zulfiqar B, Shelper TB, Avery VM (2017) Leishmaniasis drug discovery: recent progress and challenges in assay development. Drug Discov Today 22:1516–1531. https://doi.org/10.1016/j.drudis.2017.06.004